

Original Research

Transcriptomic Analysis of Cell-free Fetal RNA in the Amniotic Fluid of Vervet Monkeys (*Chlorocebus sabaesus*)

Anna J Jasinska,^{1,2,*} Dalar Rostamian,¹ Ashley T Davis,³ and Kylie Kavanagh^{3,4}

NHP are important translational models for understanding the genomic underpinnings of growth, development, fetal programming, and predisposition to disease, with potential for the development of early health biomarkers. Understanding how prenatal gene expression is linked to pre- and postnatal health and development requires methods for assessing the fetal transcriptome. Here we used RNAseq methodology to analyze the expression of cell-free fetal RNA in the amniotic fluid supernatant (AFS) of vervet monkeys. Despite the naturally high level of degradation of free-floating RNA, we detected more than 10,000 gene transcripts in vervet AFS. The most highly expressed genes were *H19*, *IGF2*, and *TPT1*, which are involved in embryonic growth and glycemic health. We noted global similarities in expression profiles between vervets and humans, with genes involved in embryonic growth and glycemic health among the genes most highly expressed in AFS. Our study demonstrates both the feasibility and usefulness of prenatal transcriptomic profiles, by using amniocentesis procedures to obtain AFS and cell-free fetal RNA from pregnant vervets.

Abbreviations: AF, amniotic fluid; AFS, AF supernatant; cffRNA, cell-free fetal RNA; hAFS, human AFS; vAFS, vervet monkey AFS

DOI: 10.30802/AALAS-CM-19-000037

Genetic and environmental factors acting during fetal development have been postulated to have long-lasting consequences on health and represent important risk factors for various diseases. For both humans and NHP, insight into the in utero environment and fetal development can be obtained from amniotic fluid (AF). Conventional AF analysis predominantly supports prenatal genetic diagnostics and biochemical assessments, for example, proteomic⁹ and neuroendocrine⁶ analyses, and, recently, as a source of fetal stem cells for modeling human diseases⁴ and regenerative medicine.¹² In addition, AF is increasingly used as a source of nucleic acids—that is, DNA and RNA—for genetic and gene expression analysis.

AF bathes numerous fetal tissues, including skin, oropharynx, lung, and the gastrointestinal and genitourinary tracts and carries transcripts expressed in these tissues. Amniotic fluid supernatant (AFS) contains cell-free fetal RNA (cffRNA), which is exclusively of fetal origin and is the biomaterial that represents gene expression purely from fetal tissues.¹⁷ Transcriptome-wide analysis of gene expression in AFS, by using either microarrays^{13,18–20,31, 40} or, more recently, RNAseq^{26,27} approaches, is increasingly applied to studies of human prenatal development and its links to health and disease.

Transcriptomic profiling of cffRNA from AF might also shed light on evolutionary differences and similarities in prenatal

development between humans and other primate species. Such a perspective would be particularly important for NHP species frequently used as models in biomedical research. Here, we performed the first comparison of AFS transcriptomes between humans and vervet monkeys (*Chlorocebus sabaesus*), which are an Old World monkey species widely used as a translational model for human disease and developmental studies.^{23,24}

Materials and Methods

Ethics statement. All animals were housed in the Vervet Research Colony at the Wake Forest School of Medicine (Winston-Salem, NC). These facilities are AAALAC-certified. The animal handling and sample collection procedures in this study were performed by a veterinarian after review and approval by the Wake Forest School of Medicine IACUC (protocol no. A15-218). Both housing and sample collection were in compliance with the US National Research Council's *Guide for Care and Use of Laboratory Animals*²¹ and meet or exceed all standards of the Public Health Service's *Policy on the Humane Care and Use of Laboratory Animals*.³⁴

Humane care guidelines. AF samples were obtained from adult female African green or vervet monkeys (*Chlorocebus sabaesus*) that are from a multigenerational pedigreed colony. Animals are descendants of 57 original founders imported from St Kitts, West Indies, and have remained a closed colony since 1985.²³ During the study, animals were housed as 16 matrilineal social groups in corrals with approximately 300 ft² indoors and 1200 ft² outdoors. Both indoor and outdoor sections were fitted with elevated perches, platforms, and climbing structures. Monkeys were fed commercial primate laboratory chow (Lab

Received: 27 Mar 2019. Revision requested: 22 Apr 2019. Accepted: 15 May 2019.

¹Center for Neurobehavioral Genetics, University of California–Los Angeles, Los Angeles, California; ²Institute of Bioorganic Chemistry, Polish Academy of Sciences, Poznan, Poland; ³Department of Pathology, Section on Comparative Medicine, Wake Forest School of Medicine, Winston-Salem, North Carolina; and ⁴Department of Biomedicine, University of Tasmania, Hobart, Australia.

*Corresponding author. Email: ankajjasinska@gmail.com

Diet no. 5038, Purina, St Louis MO) supplemented with fresh fruits and vegetables. All animals had unrestricted access to food, water, and opportunities to exercise. Group sizes ranged from 11 to 23 animals, with 1 or 2 intact adult males included in each group. Unfamiliar males are rotated into each group every 3 to 5 y.

We collected AF from 12 pregnant vervet monkeys through ultrasound-guided amniocentesis during their second and third trimesters. A volume of at least 3 mL was collected and was noted to be clear and free of gross blood contamination. The viability of the fetus was confirmed during the ultrasound examination by measuring fetal structures and assessment of heart function, as previously described.²⁸

We regularly screen the colony for SIV, simian T-lymphotropic virus, SA6 African green monkey CMV, and SA8 viruses and, except for CMV, the colony is consistently negative. CMV is not typically associated with abortion and stillbirth. All available aborted fetus, stillbirth, or neonatal death was subjected to a full pathological examination including gross and histopathological review by a veterinary pathologist. Evaluations included pathogen testing when indicated by the pathologist's review. In this study cohort, no infectious causes of death were considered present.²⁹

Sample collection and processing. The collected AF was spun down ($1000 \times g$ for 10 min at 4 °C) immediately after collection to remove residual vernix, and the supernatant (vAFS) was collected and instantaneously flash frozen by submerging in liquid nitrogen; samples subsequently were stored below -80 °C. For the transcriptomic analysis, we selected 3 samples with large volumes of vAFS (4.5 to 5 mL) and without visible blood contamination. These 3 samples were obtained from pregnancies resulting in a healthy born infant, a stillborn infant, and a single spontaneously aborted fetus (Table 1). The amniocentesis procedure was not believed to be related to stillbirth or abortion, given that factors relating to these outcomes have been examined²⁸ and the frequency of fetal loss is not higher in animals that undergo amniocentesis compared with animals that do not (data not shown).

The extraction of total RNA from the AFS samples was conducted according to a previous protocol.¹⁰ RNA was extracted within 30 to 45 d after collection. Briefly, we used a QIAamp Circulating Nucleic Acid Kit (Qiagen Sciences, Germantown, MD) for RNA isolation; after extraction and for cleanup after DNase treatment, we purified the RNA by using an RNeasy MinElute Cleanup Kit (Qiagen).

RNAseq analysis. We created cDNA libraries from 100 ng of total RNA by using the Ovation cDNA Synthesis/SPIA Amplification Kit (NuGEN Technologies, San Carlos, CA). Sequencing was conducted on a HiSeq2500 instrument by using RAPID (version 2) chemistry and generating 50-bp pair-end reads at 47.8 to 66.3 million reads per sample. The RNAseq reads were aligned to the *Chlorocebus_sabeus* 1.1 reference genomic assembly (GCF_000409795.2).⁴⁵ Our dataset is deposited in NCBI's Gene Expression Omnibus, under accession number GSE119908.

RNAseq reads were aligned to the vervet genomic assembly *Chlorocebus_sabeus* 1.1 GCF_000409795.2⁴⁵ by using the STAR aligner.¹¹ Fragment counts were derived by using HTseq.³

We conducted a comparative analysis of the vervet AFS transcriptome with similar human samples and vervet postnatal tissues for which gene expression data sets are publically available in the NCBI repository. For the comparative analysis with human AFS (hAFS), we used transcriptomic data from hAFS generated through either RNAseq (a total of 21 samples: 5 samples

from GSE49890⁴⁶ and 16 samples from GSE68180)²⁶ or by using expression microarray technology (a total of 74 samples: 14 samples from GSE16176, 11 samples from GSE25634, 12 samples from GSE33168, 16 samples from GSE46286, 16 samples from GSE48521, and 5 samples from GSE49891).^{13,19,20} For the comparative analysis with vervet postnatal tissues, we used RNAseq data that we had generated previously from 6 tissues (blood, fibroblasts, adrenal, pituitary, caudate, and hippocampus) from 59 or 60 vervets that ranged in age from neonates to adults.²⁴ The RNAseq dataset from postnatal vervet tissues is available at NCBI's Gene Expression Omnibus as bioproject PRJNA490653 (series GSE119908).

For comparative analysis of vAFS and vervet postnatal tissues (all datasets generated through RNAseq), we applied quantile normalization to all samples together. For comparative analysis of vAFS, vervet postnatal tissues, and hAFS datasets (comprising of both RNAseq and microarray datasets), we applied quantile normalization to all samples together (including 3 vervet samples and all other samples); batch effect was adjusted by using Combat.²⁵ The top 1000 most-variable genes were selected for multidimensional scaling. We conducted MDS analysis by using the plotMDS function in edgeR³⁹ to visualize the distance between the vAFS samples we analyzed herein and the reference datasets. For gene-annotation enrichment analysis, we used Database for Annotation, Visualization and Integrated Discovery (DAVID), version 6.8.¹⁶ This tool maps genes to associated biologic terms (such as Gene Ontology terms and other annotations) and identifies the most over-represented terms among the genes of interest. We used a false discovery rate of 0.05 as a threshold for enriched terms.

Results

The amniocentesis procedure typically yields 10 to 20 mL of AF from humans¹⁷ and, based on our experience, 0.75 to 5 mL (average, 3.4 mL) from vervet monkeys. vAF was separated by centrifuge into 2 fractions: AFS containing cffRNA and pellets comprising amniocytes and vernix. From 3 AFS samples, we generated cDNA libraries, which subsequently were used for the RNAseq analysis.

As expected, free-floating cffRNA, unprotected by cellular structures, showed a naturally high level of RNA degradation, with RNA integrity numbers ranging from 1.3 to 2.5 (Table 1). Because of natural cffRNA fragmentation or degradation, cDNA amplification generated transcripts smaller than average transcripts from intact RNA from cells and tissues (Figure 1). However, we still obtained usable cDNA libraries, in which we detected 23,276 genes expressed overall by using RNAseq.

Global gene expression profiles. First, we compared global expression profiles between vAFS cffRNA from 3 different pregnancies and cellular RNA from 6 postnatal vervet tissues (hippocampus, caudate, adrenal, pituitary, skin fibroblasts, and whole blood) that we had characterized previously by using RNAseq.²⁴ The first 2 dimensions from the multidimensional scaling analysis showed clear clustering according to sample type (Figure 2 A). The postnatal tissues clustered separately from each other (except for the 2 brain regions—the caudate and hippocampus—which showed a slight overlap) and distantly from a cluster of vAFS samples.

Next, we compared our vAFS samples with 95 hAFS samples from 8 datasets generated by using microarray and RNAseq (Figure 2 B). Although the global gene expression profiles from the vAFS formed a distinct cluster, which was well separated from the vervet postnatal tissues, they clustered together with both microarray and RNAseq samples from hAFS. This analysis

Table 1. Study subjects and samples selected for RNAseq analysis

Mother		Infant				AFS volume (mL)	RNA integrity number	RNA yield (ng)	No. of RNAseq reads
ID no.	Age (Y)	ID no.	Cranial diameter (cm)	Sex	Status				
2008-100	7	2015-008	2	F	stillborn	4.5	1.3	107	66,267,374
2006-020	9	2015-011	2.8	M	live	4.5	2.5	341	47,814,071
1999-034	16	2203	2.2	unknown	aborted	5	1.8	376	57,761,334

Selected females represent a range of maternal ages, but all had comparable birth outcomes (6 births, 83.3% surviving).

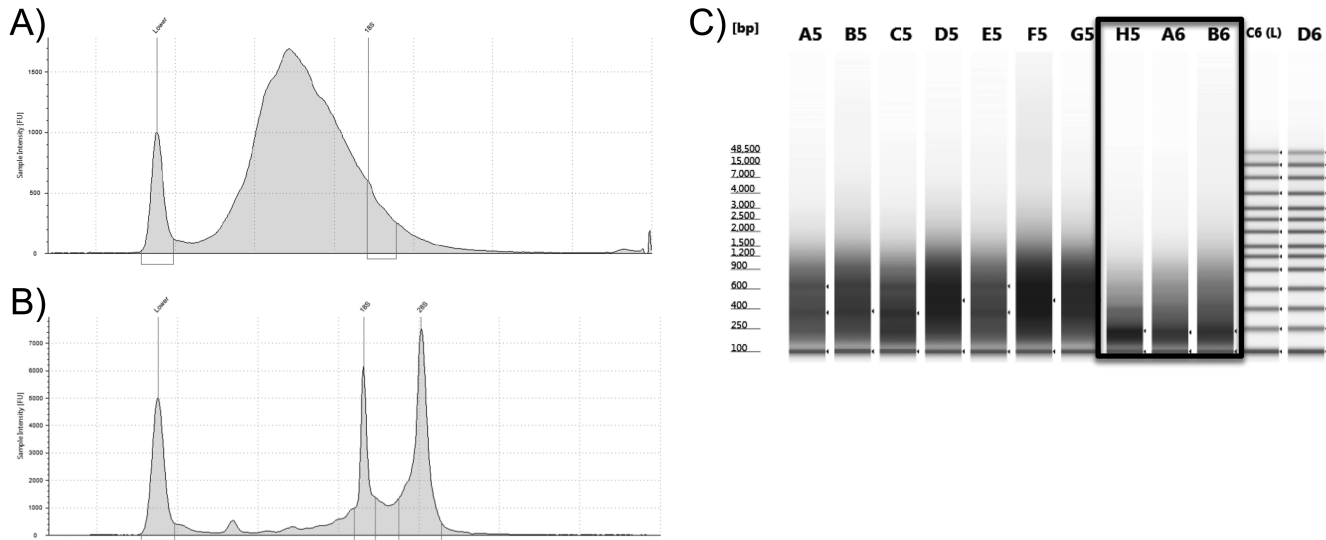


Figure 1. Quality of total RNA and cDNA libraries from cffRNA from vervet AFS. The integrity of (A) cffRNA from vervet AFS compared with (B) exceptionally high-quality total RNA. (C) cDNA libraries generated from cffRNA from vervet AFS (black frame) and from high-quality RNA.

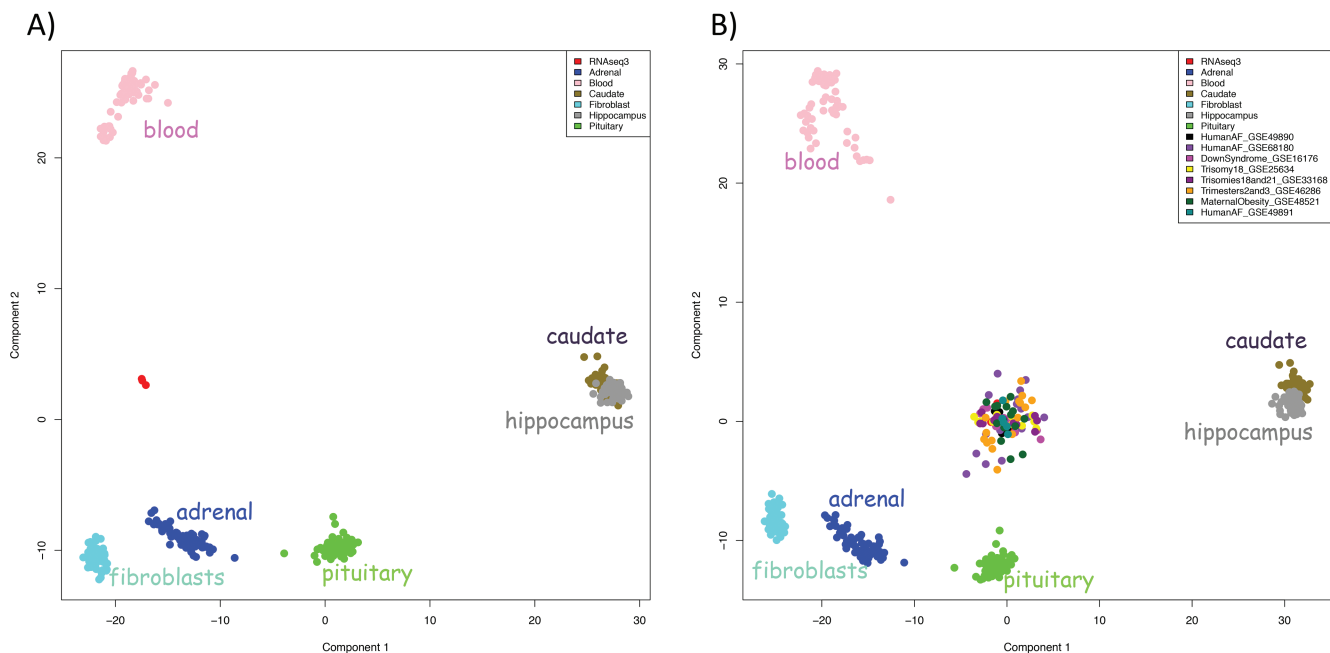


Figure 2. MDS plot of gene expression. (A) Samples generated through RNAseq of cffRNA from vervet AFS form a distinct cluster separate from samples from various vervet postnatal tissues yet (B) cluster with transcripts from human AFS samples analyzed by using both RNAseq and a microarray platform. Different colors indicate different datasets as indicated in the key (the vervet AFS samples are shown in red; they form a cluster in the center of both plots).

demonstrated that vAFS has an expression profile distinct from multiple postnatal tissues in the vervet and shows marked similarities with hAFS.

vAFS transcriptome. In vAFS, we detected 23,276 gene transcripts overall, including 10,229 gene transcripts with robust expression (that is, 1 or more fragments per kilobase

Table 2. The top 100 most-expressed genes in vervet AFS

Gene symbol	Gene description	Gene type	Rank vAFS GSE119908	Rank hAFS GSE49890	Rank hAFS GSE68180
H19	H19, imprinted maternally expressed transcript	noncoding RNA	1	N/A	N/A
IGF2	insulin like growth factor 2	protein coding	2	11	13
TPT1	tumor protein, translationally controlled 1	protein coding	3	5	42
EEF1A1	eukaryotic translation elongation factor 1 α 1	protein coding	4	20	19
RPS11	ribosomal protein S11	protein coding	5	24	27
FTL	ferritin light chain	protein coding	6	18	9
LOC103238605	40S ribosomal protein S13	protein coding	7	NA	NA
RPS6	ribosomal protein S6	protein coding	8	82	43
LOC103226991	60S ribosomal protein L31 pseudogene	pseudogene	9	NA	NA
RPS16	ribosomal protein S16	protein coding	10	85	50
VIM	vimentin	protein coding	11	146	132
LOC103227869	40S ribosomal protein S20	protein coding	12	NA	NA
RPS12	ribosomal protein S12	protein coding	13	79	46
LOC103236652	40S ribosomal protein S24 pseudogene	pseudogene	14	NA	NA
RPLP0	ribosomal protein lateral stalk subunit P0	protein coding	15	180	105
S100A6	S100 calcium binding protein A6	protein coding	16	1172	127
S100A11	S100 calcium binding protein A11	protein coding	17	35	26
LOC103233092	40S ribosomal protein S12 pseudogene	pseudogene	18	NA	NA
RPS8	ribosomal protein S8	protein coding	19	61	31
RPL24	ribosomal protein L24	protein coding	20	917	128
LOC103229159	translationally controlled tumor protein pseudogene	pseudogene	21	NA	NA
WFDC2	WAP 4-disulfide core domain 2	protein coding	22	211	171
PABPC1	poly(A) binding protein cytoplasmic 1	protein coding	23	97	53
RPS5	ribosomal protein S5	protein coding	24	95	65
RPL19	ribosomal protein L19	protein coding	25	103	69
GNB2L1	guanine nucleotide binding protein (G protein), β polypeptide 2-like 1	protein coding	26	105	87
RPS25	ribosomal protein S25	protein coding	27	108	35
RPL27	ribosomal protein L27	protein coding	28	127	92
LOC103216818	translationally-controlled tumor protein pseudogene	pseudogene	29	NA	NA
LOC103228928	elongation factor 1- α 1 pseudogene	pseudogene	30	NA	NA
LOC103216022	40S ribosomal protein S15a	pseudogene	31	NA	NA
RPL4	ribosomal protein L4	protein coding	32	199	76
S100A10	S100 calcium binding protein A10	protein coding	33	176	39
LOC103238863	uncharacterized LOC103238863	pseudogene	34	NA	NA
LOC103226548	60S ribosomal protein L5 pseudogene	pseudogene	35	NA	NA
LOC103226449	60S ribosomal protein L4-like	protein coding	36	NA	NA
ANXA1	annexin A1	protein coding	37	261	24
LOC103215865	annexin A8	protein coding	38	NA	NA
LOC103244702	40S ribosomal protein S7 pseudogene	pseudogene	39	NA	NA
RPS3	ribosomal protein S3	protein coding	40	83	190
LOC103226189	ferritin heavy chain	protein coding	41	NA	NA
LOC103216271	nucleophosmin pseudogene	pseudogene	42	NA	NA
LOC103214626	60S ribosomal protein L30	protein coding	43	NA	NA
EIF4G2	eukaryotic translation initiation factor 4 γ 2	protein coding	44	185	124
RPL7	ribosomal protein L7	protein coding	45	218	45
RPL11	ribosomal protein L11	protein coding	46	49	41
LOC103236378	40S ribosomal protein S3a	protein coding	47	NA	NA
LOC103233336	60S ribosomal protein L41	protein coding	48	NA	NA
KRT24	keratin 24	protein coding	49	681	292
ANXA2	annexin A2	protein coding	50	30	89
LOC103244020	60S ribosomal protein L23	protein coding	51	NA	NA
RPL14	ribosomal protein L14	protein coding	52	371	141

Table 2. Continued

Gene symbol	Gene description	Gene type	Rank vAFS GSE119908	Rank hAFS GSE49890	Rank hAFS GSE68180
LOC103218934	60S ribosomal protein L13 pseudogene	pseudogene	53	NA	NA
RPL27A	ribosomal protein L27a	protein coding	54	1932	648
LOC103237685	elongation factor 1- α pseudogene	pseudogene	55	NA	NA
LOC103237602	60S ribosomal protein L12	protein coding	56	NA	NA
LOC103245600	60S ribosomal protein L18	protein coding	57	NA	NA
SNAI2	snail family transcriptional repressor 2	protein coding	58	354	269
RPL10A	ribosomal protein L10a	protein coding	59	152	55
LOC103241228	putative elongation factor 1- α -like 3	pseudogene	60	NA	NA
LOC103242980	protein S100-A11 pseudogene	pseudogene	61	NA	NA
RPS20	ribosomal protein S20	protein coding	62	337	140
LOC103220002	annexin A2 pseudogene	pseudogene	63	NA	NA
PDLIM1	PDZ and LIM domain 1	protein coding	64	167	311
RPS27	ribosomal protein S27	protein coding	65	29	7
LOC103234934	40S ribosomal protein S26-like	protein coding	66	NA	NA
LOC103238540	nascent polypeptide-associated complex subunit α	protein coding	67	NA	NA
LOC103220486	40S ribosomal protein S8 pseudogene	pseudogene	68	NA	NA
RPS7	ribosomal protein S7	protein coding	69	244	144
LOC103238226	40S ribosomal protein S25 pseudogene	pseudogene	70	NA	NA
OST4	oligosaccharyltransferase complex subunit 4, noncatalytic	protein coding	71	151	40
LOC103217050	40S ribosomal protein S3a pseudogene	pseudogene	72	NA	NA
RPLP1	ribosomal protein lateral stalk subunit P1	protein coding	73	42	52
LOC103216627	40S ribosomal protein S4, X isoform-like	protein coding	74	NA	NA
ACTB	actin β	protein coding	75	28	49
EEF1G	eukaryotic translation elongation factor 1 γ	protein coding	76	69	84
RPL36AL	ribosomal protein L36a like	protein coding	77	360	148
TUBA1B	tubulin α 1b	protein coding	78	68	106
LOC103240897	60S ribosomal protein L19 pseudogene	pseudogene	79	NA	NA
LOC103221872	40S ribosomal protein S27-like	protein coding	80	NA	NA
LOC103246919	40S ribosomal protein S19	protein coding	81	NA	NA
EEF2	eukaryotic translation elongation factor 2	protein coding	82	59	98
LOC103246174	60S ribosomal protein L6	protein coding	83	NA	NA
RPL15	ribosomal protein L15	protein coding	84	236	143
SERPINB9	serpin family B member 9	protein coding	85	10611	12391
CRIP1	cysteine rich protein 1	protein coding	86	202	182
CCND2	cyclin D2	protein coding	87	224	407
TUBB	tubulin β class I	protein coding	88	204	2428
RPL28	ribosomal protein L28	protein coding	89	62	283
RPS18	ribosomal protein S18	protein coding	90	32077	206
LOC103219323	actin, cytoplasmic 1	protein coding	91	NA	NA
RPL37	ribosomal protein L37	protein coding	92	187	118
NPC2	NPC intracellular cholesterol transporter 2	protein coding	93	922	273
LOC103232182	60S acidic ribosomal protein P2 pseudogene	pseudogene	94	NA	NA
LOC103240161	60S ribosomal protein L7a-like	protein coding	95	NA	NA
LOC103241403	60S ribosomal protein L17 pseudogene	pseudogene	96	NA	NA
RPL9	ribosomal protein L9	protein coding	97	957	68
RPL17	ribosomal protein L17	protein coding	98	339	97
RPS23	ribosomal protein S23	protein coding	99	852	159
TGM2	transglutaminase 2	protein coding	100	181	508

NA, no corresponding ortholog in human annotation *Chlorocebus sabaeus* Annotation Release 100.

of transcript per 1 million mapped reads). Among the 10,229 expressed genes, 2093 genes were LOC genes, for which no human orthologs have been determined and usually with uncertain function. The list of the 100 most-expressed genes in

vAFS is presented in Table 2 the most-expressed genes were *H19*, *IGF2*, and *TPT1*.

We focused on the most expressed genes in vAFS. To assess whether any biologic functions are associated with genes highly

Table 3. Gene-term enrichment analysis results for the 500 most-expressed genes in vAFS

Category	Term	Count	P	False discovery rate
GOTERM_MF_DIRECT	GO:0003735 approximately structural constituent of ribosome	61	6.95E-65	7.33E-62
GOTERM_BP_DIRECT	GO:0006412 approximately translation	59	1.36E-56	1.49E-53
GOTERM_CC_DIRECT	GO:0005840 approximately ribosome	47	3.51E-49	3.53E-46
INTERPRO	IPR011332: Ribosomal protein, zinc-binding domain	7	1.75E-08	2.58E-05
GOTERM_CC_DIRECT	GO:0015934 approximately large ribosomal subunit	7	3.53E-07	3.55E-04
GOTERM_BP_DIRECT	GO:0006446 approximately regulation of translational initiation	7	1.15E-06	0.0012
GOTERM_CC_DIRECT	GO:0016282 approximately eukaryotic 43S preinitiation complex	6	2.52E-06	0.0025
GOTERM_CC_DIRECT	GO:0033290 approximately eukaryotic 48S preinitiation complex	6	2.52E-06	0.0025
GOTERM_CC_DIRECT	GO:0005852 approximately eukaryotic translation initiation factor 3 complex	6	2.52E-06	0.0025
GOTERM_CC_DIRECT	GO:0015935 approximately small ribosomal subunit	6	4.25E-06	0.0042
GOTERM_BP_DIRECT	GO:0001731 approximately formation of translation preinitiation complex	6	6.76E-06	0.0074

BP, biologic process; CC, cellular component; MF, molecular function

expressed in vAFS, we conducted gene-annotation analysis in the 500 most-expressed genes in vAFS. The enrichment analysis of biologic terms associated with these genes revealed that the enriched gene functions are predominantly related to ribosomes and their structural constituents, including small and large ribosomal subunits, and the processes of translation, translation initiation, and preinitiation (Table 3).

Discussion

Transcriptomic studies across development in NHP have practically been restricted to postnatal tissues collected by using minimally or moderately invasive procedures, such as blood (and sometimes fat, muscle, liver, and skin biopsies) and postmortem tissues harvested during both pre- and postnatal development.^{5,24,36} Given the importance of NHP as models for biomedical studies, it is important to expand such investigations by introducing evaluations of prenatal development that allow the linking of prenatal fetal transcriptome with potential long-term health consequences. Here we demonstrated the feasibility of characterizing fetal RNAseq profiles from cffRNA in AFS as a proxy sample for fetal gene expression in vervet monkeys, one of the most widely used NHP model species.^{22,23}

Despite the naturally high level of degradation of the free-floating cffRNA in AFS, we detected more than 10,000 genes with robustly measured expression in vervets. Gene-term enrichment analysis showed that genes with high expression were enriched for ribosomal components and translation, especially early stages of this process, which is consistent with intensive yet controlled growth and development during gestation.

Among the most highly expressed genes in vAFS were *H19* and *IGF2*. *H19* encodes a precursor of the microRNAs miR-675-5p and miR-675-3p⁷ and is associated with prenatal and early postnatal growth,^{14,37} shows tumor suppressor activity,^{15,30} and is deregulated in cancer progression, metastasis, and fetal growth syndromes.^{14,32} Deregulation of *H19* expression during development causes Beckwith–Wiedemann and Silver–Russell syndromes,^{35,41} whereas in adults, *H19* overexpression is associated with an increased risk of several cancers. *H19* is the second most-expressed transcript in placenta.³⁰ *IGF2* encodes a hormone that promotes developmental growth during gestation. *H19* and *IGF2* are both genes that are involved in embryogenesis and are reciprocally imprinted in humans: *H19* is expressed from the maternally derived allele, and *IGF2* is

expressed from the paternally derived allele.³⁸ Genetic variation in these genes is associated with low birth weight in infants.¹ In addition to genetic factors, maternal mental health during pregnancy influences *H19* and *IGF2* methylation status.^{32,44} Furthermore, intrauterine hyperglycemia is associated with alterations in the expression and methylation status of these genes.⁴²

TPT1 (also known as *TCTP*) is the third most highly expressed gene in vAFS and is among the most highly expressed genes in hAFS. This gene is crucial for pancreatic cell proliferation during embryogenesis and the adaptation of these cells in response to insulin resistance in postnatal life⁴³ and cancer development.² Knockout of *Tpt1* in mice is embryonically lethal.⁸

We observed global similarities in AFS expression profiles of vervets and humans. According to gene expression, our vAFS samples (which were analyzed with RNAseq) clustered with hAFS samples regardless of the analysis platform (both microarray and RNAseq). Importantly, *IGF2* and *TPT1*, which are involved in embryonic growth and glycemic health in humans, are among the most highly expressed genes in AFS in both humans and vervets (Table 2). Maternal glycemic health has been implicated as a risk factor associated with infant mortality in vervet monkeys.²⁸

In summary, we demonstrated the feasibility of assessing the fetal transcriptome in vervet monkeys through RNAseq analysis of cffRNA from AFS. This approach required moderately invasive sampling, which can be conducted on pregnant females in NHP breeding colonies to provide valuable insight into early developmental trajectories of fetal gene expression. AFS transcriptome is a possible source for biomarkers and predictors of the effects of genetics and early environmental exposures on prenatal and postnatal growth, development, and health.

Acknowledgments

This research was funded by a 2014 Mature pilot grant from Comparative Medicine, Wake Forest School of Medicine (to Kylie Kavanagh): “Effects of antenatal maternal factors on prenatal and postnatal development.” The Vervet Research Colony is supported by NIH grants UL1 TR001420 and P40 OD010965. Dalar Rostamian was involved in this research through the UCLA SRP99 program. We acknowledge the support of the NINDS Informatics Center for Neurogenetics and Neurogenomics (P30 NS062691). We thank Dr Matthew J Jorgensen whose contribution made this project possible.

References

- Adkins RM, Somes G, Morrison JC, Hill JB, Watson EM, Magann EF, Krushkal J. 2010. Association of Birth Weight with Polymorphisms in the IGF2, H19 and IGF2R Genes. *Pediatr Res* 68:429–434. <https://doi.org/10.1203/PDR.0b013e3181f1ca99>.
- Amson R, Pece S, Marine JC, Di Fiore PP, Teleman A. 2013. TPT1/TCTP-regulated pathways in phenotypic reprogramming. *Trends Cell Biol* 23:37–46. <https://doi.org/10.1016/j.tcb.2012.10.002>.
- Anders S, Pyl PT, Huber W. 2014. HTSeq—a Python framework to work with high-throughput sequencing data. *Bioinformatics* 31:166–169. <https://doi.org/10.1093/bioinformatics/btu638>.
- Antonucci I, Provenzano M, Rodrigues M, Pantalone A, Salini V, Ballerini P, Borlongan CV, Stuppia L. 2016 Amniotic fluid stem cells: a novel source for modeling of human genetic diseases. *Int J Mol Sci* 17: 1–14. <https://doi.org/10.3390/ijms17040607>
- Bakken TE, Miller JA, Ding SL, Sunkin SM, Smith KA, Ng L, Szafer A, Dalley RA, Royall JJ, Lemon T, Shapouri S, Aiona K, Arnold J, Bennett JL, Bertagnolli D, Bickley K, Boe A, Brouner K, Butler S, Byrnes E, Caldejon S, Carey A, Cate S, Chapin M, Chen J, Dee N, Desta T, Dolbeare TA, Dotson N, Ebbert A, Fulfs E, Gee G, Gilbert TL, Goldy J, Gourley L, Gregor B, Gu G, Hall J, Haradon Z, Haynor DR, Hejazinia N, Hoerder-Suabedissen A, Howard R, Jochim J, Kinnunen M, Kriedberg A, Kuan CL, Lau C, Lee CK, Lee F, Luong L, Mastan N, May R, Melchor J, Mosqueda N, Mott E, Ngo K, Nyhus J, Oldre A, Olson E, Parente J, Parker PD, Parry S, Pendergraft J, Potekhina L, Reding M, Riley ZL, Roberts T, Rogers B, Roll K, Rosen D, Sandman D, Sarreal M, Shapovalova N, Shi S, Sjoquist N, Sodt AJ, Townsend R, Velasquez L, Wagley U, Wakeman WB, White C, Bennett C, Wu J, Young R, Youngstrom BL, Wohnoutka P, Gibbs RA, Rogers J, Hohmann JG, Hawrylycz MJ, Hevner RF, Molnár Z, Phillips JW, Dang C, Jones AR, Amaral DG, Bernard A, Lein ES. 2016. A comprehensive transcriptional map of primate brain development. *Nature* 535:367–375. <https://doi.org/10.1038/nature18637>.
- Baron-Cohen S, Auyeung B, Nørgaard-Pedersen B, Hougaard DM, Abdallah MW, Melgaard L, Cohen AS, Chakrabarti B, Ruta L, Lombardo MV. 2015. Elevated fetal steroidogenic activity in autism. *Mol Psychiatry* 20:369–376. <https://doi.org/10.1038/mp.2014.48>.
- Cai X, Cullen BR. 2007. The imprinted H19 noncoding RNA is a primary microRNA precursor. *RNA* 13:313–316. <https://doi.org/10.1261/rna.351707>.
- Chen SH, Wu PS, Chou CH, Yan YT, Liu H, Weng SY, Yang-Yen HF. 2007. A knockout mouse approach reveals that TCTP functions as an essential factor for cell proliferation and survival in a tissue- or cell type-specific manner. *Mol Biol Cell* 18:2525–2532. <https://doi.org/10.1091/mbc.e07-02-0188>.
- Cho CK, Shan SJ, Winsor EJ, Diamandis EP. 2007. Proteomics analysis of human amniotic fluid. *Mol Cell Proteomics* 6: 1406–1415.
- Dietz JA, Johnson KL, Massingham LJ, Schaper J, Horlitz M, Cowan J, Bianchi M. 2011. Comparison of extraction techniques for amniotic fluid supernatant demonstrates improved yield of cell-free fetal RNA. *Prenat Diagn* 31:598–599. <https://doi.org/10.1002/pd.2732>.
- Dobin A, Davis CA, Schlesinger F, Drenkow J, Zaleski C, Jha S, Batut P, Chaisson M, Gingeras TR. 2012. STAR: ultrafast universal RNAseq aligner. *Bioinformatics* 29:15–21. <https://doi.org/10.1093/bioinformatics/bts635>.
- Dziadosz M, Basch RS, Young BK. 2016. Human amniotic fluid: a source of stem cells for possible therapeutic use. *Am J Obstet Gynecol* 214:321–327. <https://doi.org/10.1016/j.ajog.2015.12.061>.
- Edlow AG, Vora NL, Hui L, Wick HC, Cowan JM, Bianchi DW. 2014. Maternal obesity affects fetal neurodevelopmental and metabolic gene expression: a pilot study. *PLoS One* 9:1–11. <http://dx.plos.org/10.1371/journal.pone.0088661>.
- Gabory A, Jammes H, Dandolo L. 2010. The H19 locus: role of an imprinted non-coding RNA in growth and development. *Bioessays* 32:473–480. <https://doi.org/10.1002/bies.200900170>.
- Hao Y, Crenshaw T, Moulton T, Newcomb E, Tycko B. 1993. Tumour-suppressor activity of H19 RNA. *Nature* 365:764–767. <https://doi.org/10.1038/365764a0>.
- Huang DW, Sherman BT, Lempicki RA. 2009. Systematic and integrative analysis of large gene lists using DAVID bioinformatics resources. *Nat Protoc* 4:44–57. <https://doi.org/10.1038/nprot.2008.211>.
- Hui L, Bianchi DW. 2013. Recent advances in the prenatal interrogation of the human fetal genome. *Trends Genet* 29:84–91. <https://doi.org/10.1016/j.tig.2012.10.013>.
- Hui L, Slonim DK, Wick HC, Johnson KL, Bianchi DW. 2012. The amniotic fluid transcriptome: a source of novel information about human fetal development. *Obstet Gynecol* 119:111–118. <https://doi.org/10.1097/AOG.0b013e31823d4150>.
- Hui L, Slonim DK, Wick HC, Johnson KL, Koide K, Bianchi DW. 2012. Novel neurodevelopmental information revealed in amniotic fluid supernatant transcripts from fetuses with trisomies 18 and 21. *Hum Genet* 131:1751–1759. <https://doi.org/10.1007/s00439-012-1195-x>.
- Hui L, Wick HC, Edlow AG, Cowan JM, Bianchi DW. 2013. Global gene expression analysis of term amniotic fluid cell-free fetal RNA. *Obstet Gynecol* 121:1248–1254. <https://doi.org/10.1097/AOG.0b013e318293d70b>.
- Institute for Laboratory Animal Research. 1985. Guide for the care and use of laboratory animals. p 85–123. Washington (DC): Department of Health and Human Services.
- Jasinska AJ. 2019. Biological resources for genomic investigation in the vervet monkey (*Chlorocebus*). p 16–28. In: Turner T, Schmitt C, Cramer J. *Savanna monkeys: The genus chlorocebus*. Cambridge University Press. <http://dx.doi.org/10.1017/9781139019941.002>
- Jasinska AJ, Schmitt CA, Service SK, Cantor RM, Dewar K, Jentsch JD, Kaplan JR, Turner TR, Warren WC, Weinstock GM, Woods RP, Freimer NB. 2013. Systems biology of the vervet monkey. *ILAR J* 54:122–143. <https://doi.org/10.1093/ilar/ilt049>.
- Jasinska AJ, Zelaya I, Service SK, Peterson CB, Cantor RM, Choi O-W, DeYoung J, Eskin E, Fairbanks LA, Fears S, Furterer A, Huang YS, Ramensky V, Schmitt CA, Svardal H, Jorgensen MJ, Kaplan JR, Villar D, Aken BL, Flicek P, Nag R, Wong ES, Blangero J, Dyer TD, Bogomolov M, Benjamini Y, Weinstock GM, Dewar K, Sabatti C, Wilson RK, Jentsch JD, Warren W, Coppola G, Woods RP, Freimer NB. 2017. Genetic variation and gene expression across multiple tissues and developmental stages in a nonhuman primate. *Nat Genet* 49:1714–1721. <https://doi.org/10.1038/ng.3959>.
- Johnson WE, Li C, Rabinovic A. 2007. Adjusting batch effects in microarray expression data using empirical Bayes methods. *Biostatistics* 8:118–127. <https://doi.org/10.1093/biostatistics/kxj037>.
- Kamath-Rayne BD, Du Y, Hughes M, Wagner EA, Muglia LJ, DeFranco EA, Whitsett JA, Salomonis N, Xu Y. 2015. Systems biology evaluation of cell-free amniotic fluid transcriptome of term and preterm infants to detect fetal maturity. *BMC Med Genomics* 8:1–11. <https://doi.org/10.1186/s12920-015-0138-5>.
- Kang JH, Park HJ, Jung YW, Shim SH, Sung SR, Park JE, Cha DH, Ahn EH. 2015. Comparative transcriptome analysis of cell-free fetal RNA from amniotic fluid and RNA from amniocytes in uncomplicated pregnancies. *PLoS One* 10:1–13. <http://dx.plos.org/10.1371/journal.pone.0132955>.
- Kavanagh K, Dozier BL, Chavanne TJ, Fairbanks LA, Jorgensen MJ, Kaplan JR. 2011. Fetal and maternal factors associated with infant mortality in vervet monkeys. *J Med Primatol* 40:27–36. <https://doi.org/10.1111/j.1600-0684.2010.00441.x>.
- Kendzierski JA, Sherrill C, Davis AT, Kavanagh K. 2019. Microbial translocation into amniotic fluid of vervet monkeys is common and unrelated to adverse infant outcomes. *J Med Primatol* 48:367–369. <https://doi.org/10.1111/jmp.12432>.
- Keniry A, Oxley D, Monnier P, Kyba M, Dandolo L, Smits G, Reik W. 2012. The H19 lincRNA is a developmental reservoir of miR-675 that suppresses growth and Igf1r. *Nat Cell Biol* 14:659–665. <https://doi.org/10.1038/ncb2521>.
- Larrabee PB, Johnson KL, Lai C, Ordovas J, Cowan JM, Tantravahi U, Bianchi DW. 2005. Global gene expression analysis of the living human fetus using cell-free messenger RNA in amniotic fluid. *JAMA* 293:836–842. <https://doi.org/10.1001/jama.293.7.836>.
- Mansell T, Novakovic B, Meyer B, Rzehak P, Vuillermin P, Ponsonby A-L, Collier F, Burgner D, Saffery R, Ryan J, BIS

- Investigator team.** 2016. The effects of maternal anxiety during pregnancy on IGF2/H19 methylation in cord blood. *Transl Psychiatry* **6**:1–7. <https://doi.org/10.1038/tp.2016.32>.
33. **Matouk IJ, Halle D, Raveh E, Gilon M, Sorin V, Hochberg A.** 2016. The role of the oncofetal H19 lncRNA in tumor metastasis: orchestrating the EMT-MET decision. *Oncotarget* **7**:3748–3765. <https://doi.org/10.18632/oncotarget.6387>.
34. **Office of Laboratory Animal Welfare.** 2019. PHS policy on humane care and use of laboratory animals. [Cited 13 January 2020]. Available at: <https://olaw.nih.gov/policies-laws/phs-policy.htm>.
35. **Okamoto K, Morison IM, Taniguchi T, Reeve AE.** 1997. Epigenetic changes at the insulin-like growth factor II/H19 locus in developing kidney is an early event in Wilms tumorigenesis. *Proc Natl Acad Sci USA* **94**:5367–5371. <https://doi.org/10.1073/pnas.94.10.5367>.
36. **Peng X, Thierry-Mieg J, Thierry-Mieg D, Nishida A, Pipes L, Bozinovski M, Thomas MJ, Kelly S, Weiss JM, Raveendran M, Muzny D, Gibbs RA, Rogers J, Schroth GP, Katze MG, Mason CE.** 2015. Tissue-specific transcriptome sequencing analysis expands the non-human primate reference transcriptome resource (NHPRT). *Nucleic Acids Res* **43** D1:D737–D742. <https://doi.org/10.1093/nar/gku1110>.
37. **Petry CJ, Seear RV, Wingate DL, Acerini CL, Ong KK, Hughes IA, Dunger DB.** 2011. Maternally transmitted foetal H19 variants and associations with birth weight. *Hum Genet* **130**:663–670. <https://doi.org/10.1007/s00439-011-1005-x>.
38. **Reik W, Walter J.** 2001. Genomic imprinting: parental influence on the genome. *Nat Rev Genet* **2**:21–32. <https://doi.org/10.1038/35047554>.
39. **Robinson MD, McCarthy DJ, Smyth GK.** 2010. edgeR: a Bioconductor package for differential expression analysis of digital gene expression data. *Bioinformatics* **26**:139–140. <https://doi.org/10.1093/bioinformatics/btp616>.
40. **Slonim DK, Koide K, Johnson KL, Tantravahi U, Cowan JM, Jarrah Z, Bianchi DW.** 2009. Functional genomic analysis of amniotic fluid cell-free mRNA suggests that oxidative stress is significant in Down syndrome fetuses. *Proc Natl Acad Sci USA* **106**:9425–9429. <https://doi.org/10.1073/pnas.0903909106>.
41. **Steenman MJ, Rainier S, Dobry CJ, Grundy P, Horon IL, Feinberg AP.** 1994. Loss of imprinting of IGF2 is linked to reduced expression and abnormal methylation of H19 in Wilms' tumour. *Nat Genet* **7**:433–439. <https://doi.org/10.1038/ng0794-433>. Erratum: *Nat Genet* 1994 **8**:203.
42. **Su R, Wang C, Feng H, Lin L, Liu X, Wei Y, Yang H.** 2016. Alteration in expression and methylation of IGF2/H19 in placenta and umbilical cord blood are associated with macrosomia exposed to intrauterine hyperglycemia. *PLoS One* **11**:1–14. <http://dx.plos.org/10.1371/journal.pone.0148399.d>
43. **Tsai M-J, Yang-Yen H-F, Chiang M-K, Wang M-J, Wu S-S, Chen S-H.** 2014. TCTP is essential for β -cell proliferation and mass expansion during development and β -cell adaptation in response to insulin resistance. *Endocrinology* **155**:392–404. <https://doi.org/10.1210/en.2013-1663>.
44. **Vangeel EB, Izzi B, Hompes T, Vansteelandt K, Lambrechts D, Freson K, Claes S.** 2015. DNA methylation in imprinted genes IGF2 and GNASXL is associated with prenatal maternal stress. Abstracts of the 45th annual meeting of the International Society of Psychoneuroendocrinology Stress and the Brain: From Fertility to Senility John McIntyre Conference Centre, Edinburgh, 8–10 September 2015. *Psychoneuroendocrinology*. **61**:16. <https://doi.org/10.1016/j.psyneuen.2015.07.430>
45. **Warren WC, Jasinska AJ, García-Pérez R, Svoldal H, Tomlinson C, Rocchi M, Archidiacono N, Capozzi O, Minx P, Montague MJ, Kyung K, Hillier LW, Kremitzki M, Graves T, Chiang C, Hughes J, Tran N, Huang Y, Ramensky V, Choi OW, Jung YJ, Schmitt CA, Juretic N, Wasserscheid J, Turner TR, Wiseman RW, Tuscher JJ, Karl JA, Schmitz JE, Zahn R, O'Connor DH, Redmond E, Nisbett A, Jacquelin B, Müller-Trutwin MC, Brenchley JM, Dione M, Antonio M, Schroth GP, Kaplan JR, Jorgensen MJ, Thomas GW, Hahn MW, Raney BJ, Aken B, Nag R, Schmitz J, Churakov G, Noll A, Stanyon R, Webb D, Thibaud-Nissen F, Nordborg M, Marques-Bonet T, Dewar K, Weinstock G, Wilson RK, Freimer NB.** 2015. The genome of the vervet (*Chlorocebus aethiops sabaues*). *Genome Res* **25**:1921–1933. <https://doi.org/10.1101/gr.192922.115>.
46. **Zwemer LM, Hui L, Wick HC, Bianchi DW.** 2014. RNAseq and expression microarray highlight different aspects of the fetal amniotic fluid transcriptome. *Prenat Diagn* **34**:1006–1014. <https://doi.org/10.1002/pd.4417>.